



LAWRENCE
LIVERMORE
NATIONAL
LABORATORY

LLNL-TR-860812

FY24Q1 VTO Quarter Report on 3D Printing of All-Solid-State Lithium Batteries

J. Ye

February 23, 2024

Disclaimer

This document was prepared as an account of work sponsored by an agency of the United States government. Neither the United States government nor Lawrence Livermore National Security, LLC, nor any of their employees makes any warranty, expressed or implied, or assumes any legal liability or responsibility for the accuracy, completeness, or usefulness of any information, apparatus, product, or process disclosed, or represents that its use would not infringe privately owned rights. Reference herein to any specific commercial product, process, or service by trade name, trademark, manufacturer, or otherwise does not necessarily constitute or imply its endorsement, recommendation, or favoring by the United States government or Lawrence Livermore National Security, LLC. The views and opinions of authors expressed herein do not necessarily state or reflect those of the United States government or Lawrence Livermore National Security, LLC, and shall not be used for advertising or product endorsement purposes.

This work performed under the auspices of the U.S. Department of Energy by Lawrence Livermore National Laboratory under Contract DE-AC52-07NA27344.

Please DO NOT CUT/PASTE OVER THESE FIRST PAGE SECTIONS.

We are trying to preserve ongoing editing to this first page by the Program Manager's team.

Instead, just make any changes directly to this page as needed.

Task 1.6 – Three-Dimensional Printing of All-Solid-State Lithium Batteries (Jianchao Ye, Lawrence Livermore National Laboratory)

Objectives. The project has two primary objectives: (1) down select three-dimensional (3D) printing and post-processing approaches for solid-state electrolyte (SSE) / cathode integration, and (2) understand battery failure mechanisms via *ex situ* and *in situ* characterization.

Impact. The adoption of a thin separator layer, thick cathode structure, and metallic lithium anode will lead to electric vehicle batteries with > 350 Wh/kg energy density for increased mileage per charge. The higher ionic conductivity with suppression of lithium dendrite growth will allow high critical current densities for fast charging applications. The improved electrode/electrolyte contact will increase battery cycle life for long-term service.

Approach. The technical approaches include advanced manufacturing based on 3D printing and related techniques, *ex situ* / *in situ* characterizations, and battery testing. Direct-ink writing 3D-printing techniques will be employed to fabricate thin-film SSEs (< 100 μm), bilayer SSEs, and 3D interfaces for battery performance evaluation. Three approaches, including sintering-free, hybrid, and co-sintering, will be investigated. The knowledge obtained from these approaches is transferable and complementary to each technique.

Out-Year Goals. The long-term vision of the team is to 3D-print all components of the all-solid-state lithium battery (ASSLB) to facilitate the scale-up of ASSLB manufacturing. In this project, the team will tackle the issues emerging from integrating solid electrolyte (SE) with electrodes. The project goal is to demonstrate a successful 3D-printing approach to integrate SSE into electrodes and show reasonable capacity retention (that is, $> 80\%$) after 300 cycles at current density ≥ 1 mA/cm^2 .

Collaborations. The team will work closely with a computational partner (Task 3.8 led by B. Wood) to better understand battery failure mechanisms and design new battery architectures and chemistries for performance improvement.

Milestones

1. Determine the effect of 3D printing on the rate performance of SSBs. (Q1 FY 2024; Completed)
2. Incorporate 3D printed separator in SSBs for enhanced stability. (Q2, FY 2024; In progress)
3. In situ monitor the involved electro-chemo-mechanical phenomena. (Q3, FY 2024; On schedule)
4. Summarize degradation mechanisms and mitigation strategies in 3D printed SSBs. (Q4, FY 2023; On schedule)

Progress Report

Switching to water base LiFePO4 (LFP) ink prevented damage to the cathode structure, leading to higher capacity of both tape-casted and 3D printed electrodes. In previous studies, the team discovered that the LFP/PVDF/CB cathode is not compatible with the composite polymer electrolyte ink recipe (CPE7, 1PEGDA/8PEGMEA/1PEO/3.3LiTFSI with 7wt% LLZTO) due to the attack of PVDF binder by acetonitrile. They therefore switched to water based LFP ink with hydroxyethyl-cellulose binder that does not dissolve in acetonitrile. The derived new electrodes were used directly to infill with composite polymer electrolyte (CPE), without additional calendering to strengthen the electrode integrity. The 3D LFP cell can now be cycled with a capacity of 140 mAh/g in contrast to failed trials with NMP/PVDF recipe. The new ink can be extruded from 100 μm nozzles, resulting in line width less than 100 μm .

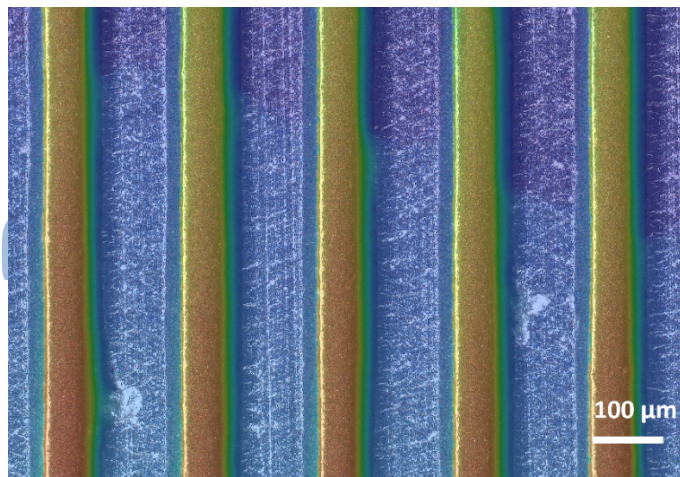


Figure 1. LFP/cellulose/CB parallel lines printed using Direct Ink Writing with 100 μm nozzle.

More than a hundred structured LFP samples were printed, among which twenty-four 3D printed samples were infilled, and thirty-nine cells were assembled and tested to evaluate the structural and chemical effects. The team generated a variety of 3D geometries from 1-layer parallel lines, 2-layer overlayed parallel lines, 2-layer grids, and 3-layer overlayed parallel lines. They also improved the Al foil mounting methods in 3D printing, which enabled prints on pre-tape-casted and dried electrode films. Two nozzle sizes were used for printing: 200 μm and 100 μm in diameter. Two ink compositions with 90% and 85% LFP were used to tune the electrical properties. Large quantities of samples were prepared to cover a broad range of geometries and compositions to help discover promising regions with improved battery performance. Figures 2a-f shows optical images of representative prints. Figure 2g shows stacks of CPEs (SPE, CPE7 and CPE7F) infilled 3D and 2D LFP electrodes. SPE stands for solid polymer electrolyte from PEGDA/PEGMEA/PEO/LiTFSI without LLZTO filler. CPE7F is modified from CPE7 by adding 1wt% FEC before UV curing. Coin cells were assembled using Li chip as anode. To avoid hard short circuit caused by weak mechanical properties of SPE and CPE7 at 60 $^{\circ}\text{C}$, additional SPE separator and CPE7-infilled porous HDDA membrane layer were inserted, respectively. For cells without additional freestanding separator, larger LFP electrodes (10mm) than Li chips (8mm) were used to avoid short circuit from edge. That arbitrarily increased the specific capacity calculated using the area directly against Li, but was still valuable to compare between different geometrical designs. To make the specific capacity calculation more accurate, a larger CPE7F freestanding film was used between same sized anode and cathode layers in recently assembled cells.

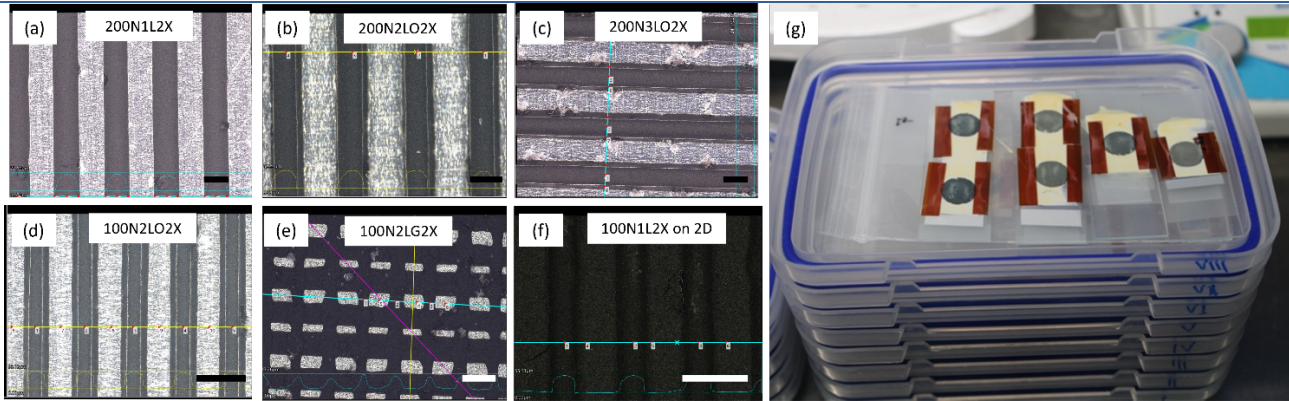


Figure 2. (a-f) Top view of representative 3D printed LFP patterns. For example, 200N2L02X means 200 μm nozzle diameter, two layer overlapping print with hatch spacing of 2 times of nozzle diameter. 100N2LG2X means 100 μm nozzle diameter, two layer grid print with hatch spacing of 2 times of nozzle diameter. **(g)** Stacks of samples after infilling with UV curable polymer electrolytes. Scale bars in (a-f) are 200 μm .

CPE7F shows higher electrochemical stability than either CPE7 or SPE. We have previously observed that the stability of CPE7 with Li can be improved by the addition of 1wt% FEC. New results shown in Figure 3a further confirmed the observation. The sample labeled as “3D LFP, 85LFP-200N2L02X, 3.57 mg/cm^2 ”, “3D LFP, 85LFP-**200N2L02X**200N2LG2X, 11.82 mg/cm^2 ”, and “2D LFP, 85LFP, 4.83 mg/cm^2 ” were infilled with CPE7F. The one labeled as “3DLFP, 90LFP-100N2L02X, 3.70 mg/cm^2 ” was infilled with CPE7. Although CPE7F possesses lower ionic conductivity, the capacity decay with cycling is much slower than CPE7. Figure 3b shows that CPE7F exhibits higher coulombic efficiency and therefore more stable than the corresponding solid polymer electrolyte (SPE) without LLZTO and FEC, even though they have similar mechanical stiffness and ionic conductivity at room temperature. The above findings confirmed the beneficial role of FEC additive in stabilizing the interfaces.

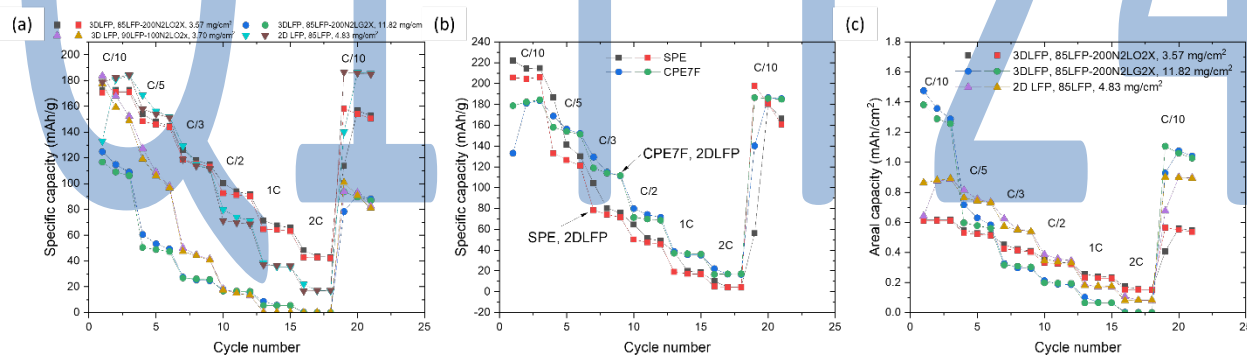


Figure 3. Rate performance testing of 3D and 2D LFP samples infilled with CPE7, CPE7F, and SPE. (a) all LFP electrodes were infilled with CPE7F except the 90LFP one with 3.70 mg/cm^2 mass loading. 10mm infilled LFP cathode discs and 8mm Li chips were used in coin cells. C-rates were set based on theoretical capacity of 170 $\text{mAh}/\text{g}_{\text{LFP}}$. (b) Comparison of rate performance between SPE and CPE7F infilled 2D LFP electrodes. (c) Mass loading effects on the areal capacity in rate performance tests.

Smaller printed feature size or thinner film helps with ionic and electronic transport. The results in Figure 3c also revealed that 3D printed electrodes with thinner lines (or smaller mass loading) show higher rate performance, suggesting the ion transport is limiting the cell kinetics. However, for thicker electrodes (higher mass loading) run at high C-rates, the areal capacity is even lower than the thinner electrodes, suggesting that electronic transport starts to play a role at high C-rates. Therefore, improving the ionic and electronic conductivities are essential to achieve high power density of all-solid-state batteries.

CPE7/CPE7F bilayer design improves initial capacity at relatively lower C-rates, while less effects at higher C-rates. Although CPE7 was proven to be incompatible with metallic lithium, it is not clear whether it

is stable LFP cathode. Given its higher ionic conductivity, it may be beneficial to use it as catholyte. Therefore, the team assembled CPE7 infilled LFP with freestanding CPE7F separator and Li anode. This time, the area of LFP and Li electrodes were the same. As shown in Figure 4, at C/10 rate, the capacity of CPE7 infilled LFP achieved over 140 mAh/g, which is similar as the LFP-Li cell with Gen-2 liquid electrolyte, suggesting most of the LFP in the solid cell is accessible. The EIS plots of the as-assembled cells clearly show a small bulk and interfacial resistance of the Li|CPE7F|CPE7-LFP compared with Li|CPE7F|CPE7F-LFP cell. As a result, the capacity of CPE7-LFP at C-rates from C/10 to C/2 is higher than CPE7F-LFP. The observation was confirmed in all other cells with similar LFP mass loadings (Figure 5). At C-rates of 1C and 2C, the improvement is however no longer apparent. After high-rate test, the cell capacity mostly recovered for CPE7F infilled cells. However, CPE7 infilled ones still exhibit a certain percentage of capacity reduction. This is consistent with the interfacial resistance increase observed in EIS plots after the rate test (Figure 4b). Long-term cycling stability will be evaluated in the next quarter.

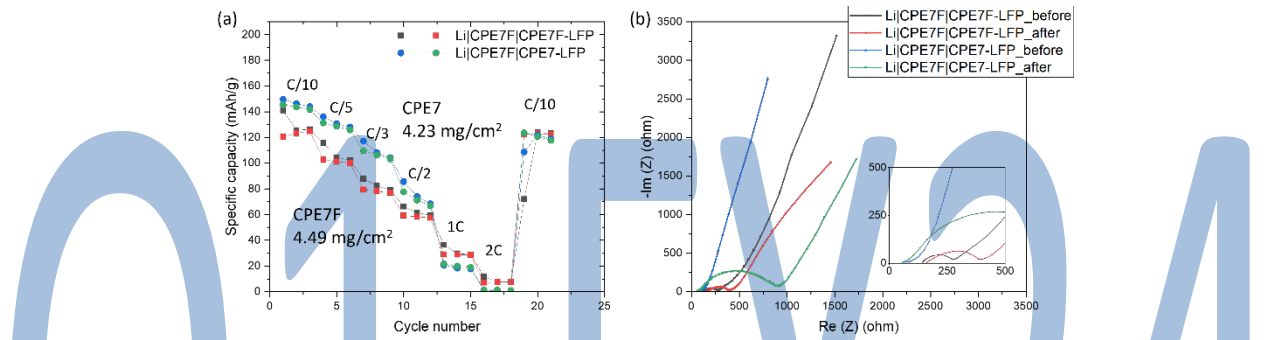


Figure 4. Rate performance (a) and EIS plots (b) of 3D printed LFP electrodes infilled with CPE7 and CPE7F. 3D printed LFP electrodes were both 90LFP-100N2LO2X.

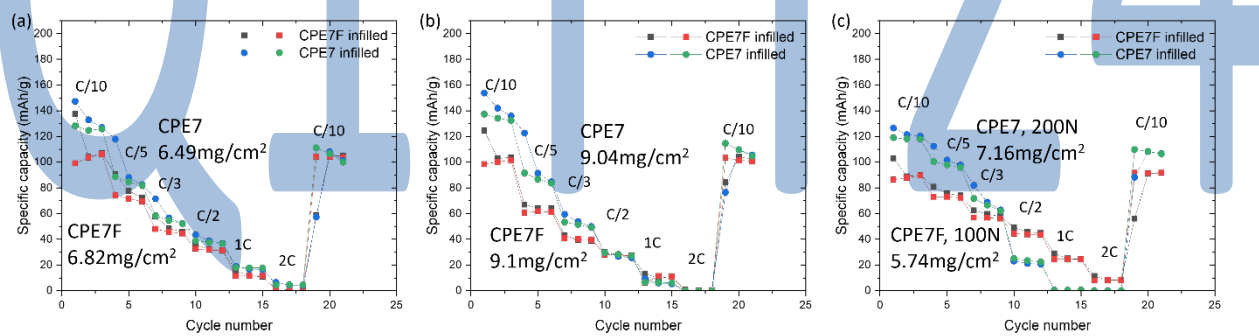


Figure 5. Comparison of rate performance of 3D printed LFP electrodes infilled with CPE7 and CPE7F. (a) CPE7F infilled 3D LFP, 85LFP-200N2LO2X vs CPE7 infilled 3D LFP, 85LFP-200N2LG2X. (b) CPE7F infilled 3D LFP, 85LFP-200N2LG2X vs CPE7 infilled 3D LFP, 85LFP-200N1LG2X. (c) CPE7F infilled 2.5DLFP, 85LFP-100N1LG2X vs CPE7 infilled 2.5D LFP, 85LFP-200N1LG2X.

Patents/Publications/Presentations

The project has no patents, publications, or presentations to report this quarter.

Q1 FY24

